Piezoelectric-Magnetostrictive Vibration Absorbers : Modelling and Optimisation

Payam Soltani
School of Engineering and the Built Environment
Birmingham City University
Birmingham,UK
ORCID:0000-0002-8186-2678

Morteza Mohammadzaheri
School of Engineering and the Built Environment
Birmingham City University
Birmingham,UK
ORCID:0000-0002-8187-6375

Mojtaba Ghodsi
School of Energy & Electronic Engineering
University of Portsmouth
Portsmouth, UK
ORCID: 0000-0002-8762-9498

***Abstract*—In this research, a new type of hybrid vibration absorber termed as the Piezoelectric-Magnetostrictive Vibration Absorber (PMVA) is introduced. The mathematical governing equations are derived and the parametric receptance function of the host strucutre is developed. The h_∞ optimisation is employed to tune the resonating shunt circuits, attached to the piezoelectric and magnetostrictive elements of the absorber using the equal-peak method. An improved dynamic coupling between the PMVA and the host structure is achieved. The performance enhancement is confirmed by the numerical results, demonstrating that the performance of the introduced PMVA could be enhanced by at least 19% in passive vibration control of the host structure compared to that of typical piezoelectric or magnetostrictive vibration absorbers. The optimum parameters of the shunt circuits at different coupling conditions are presented, which can be used for further applications of this new type of absorber.**

***Index Terms*—Vibration Absorbers, Piezoelectric Absorbers, Magnetostrictive Absorbers, h_∞ optimisation**

I. Introduction

Vibration absorbers are auxiliary resonating systems that are coupled to a vibrating host structure with the aim of extracting a portion of the kinetic energy of the host and reducing its amplitude of vibration. These auxiliary systems can take different forms and types. Mechanical vibration absorbers usually consist of resonating mechanical structures, such as mass-spring systems or pendulums [1], [2], or a resonating fluid flow within a U-shaped pipe [3]. These mechanical absorbers are widely used in passive vibration control of tall buildings [4], skyscrapers [5], bridges [6], wind turbine towers [7], or even suspension systems of vehicles [8]. However, adding new mechanical auxiliary absorbers to the host structure and adjusting their components to match the vibrating characteristics of the host is not always an easy task and may not be practically feasible for all systems, which significantly limits the application of mechanical absorbers.

Electromechanical systems can be used also as the auxiliary resonating vibration absorbers, coupled to the host structure. Piezoelectric (PZT) elements attached to a resonating shunt circuit (usually an RLC circuit) , create a Piezoelectric Vibration Absorber (PVA), which provides an alternative solution to mechanical absorbers. [9], [10]. A network of PZT patches or rods can be attached to, coupled with, and/or embedded in the host structure, and thanks to the piezoelectric characteristics of PZT transducers, a part of the kinetic energy of the host (the main structure) is transformed into electrical energy within the shunt circuit. This leads to effective vibration control of the host. However, the shunt circuit of the PVA needs to be tuned to maximise its attenuating performance, achieved through the proper choice of shunt circuit elements, i.e. optimum values of resistance, inductance, and capacitance [10]. Tuning the shunt circuit, especially when using digital electrical circuits, is much easier than tuning a mechanical one, making the PVA an ideal candidate for vibration control of lightweight structures. Tuned PVAs have found extensive and successful applications in various industries and practical problems where reducing unwanted vibrations is critical to improving performance outcomes, accuracy, and user experience [11]. Applications such as vibration control of wings [12] and antennas in spacecrafts [13], vibration reduction in hard disk drivers [14], composite structures [15] , submerged [11], and brake systems [16] . Moreover, tuned PVAs are employed in different components of sensitive robots such as the gripper, body, and arms , where unwanted vibration may result in errors in positioning and performance of the robot [17]. Shunted PVAs are also widely used in noise reduction of systems and structures [18] such as sandwich panels [19] , ducts [20] and railway wheels [21].

Magnetostrictive (MAG) transducers such as terbium-iron-dysprosium alloys (Terfenol-D) [22], [23] and iron-gallium alloys (Galfenol) [24], [25] can be also coupled to a resonating shunt circuit adjacent to a permanent magnet and through an induction coil closely wound around MAG to create a Magnetostrictive Vibration Absorber (MVA) [26], [27]. The MVA can be coupled to a host structure to convert excessive vibrations of the host into magnetic energy first, which is then dissipated via heat loss, hysteresis, and eddy currents in the

shunt circuit. The use of MVAs has advantageous due to their relatively appropriate level of magnetomechanical coupling factor [28] and high relatability [29] allowing for efficient energy conversion from the mechanical system to the electrical shunt. The resonant frequency of the MVA can be tuned to match the frequency of the vibration source to maximise the absorption of vibration energy. Additionally, the MVA can be designed to be compact, lightweight, and able to withstand high-temperature environments, making them suitable for use in various applications. They are being used in vibration suspension of different systems and structures such as rotary machines [30] , wind turbine blade and tower [31] and micro-vibration suppression [32] .

One of the major challenges in the application of dynamic absorbers is designing a system that efficiently couples the auxiliary mechanism (the dynamic absorber) with the vibrating host. Higher dynamic coupling facilitates energy transfer between these two systems, resulting in a better attenuating performance and absorber efficiency. To enhance dynamic coupling, one possible solution is to use a series and/or network of vibration absorbers instead of a single one. This method has been widely investigated and applied for different types of absorbers, such as MVAs and PVAs. However, designing an optimum network of absorbers and the way they are coupled and attached to the main structure is still an ongoing research topic. This approach is highly dependent on the shape, resonant frequency, and material properties of the host, as well as the energy conversion characteristics of the absorbers. These challenges make this solution a complex methodology to combat the issue of enhancing the dynamic coupling between vibrating systems in proposing the optimum design of dynamic absorbers. An alternative solution , is combining different types of energy conversion transducers, such as PZT and MAG elements, to create a hybrid smart energy conversion cell that can be coupled to the host structure and enhances the dynamic coupling between the mechanical structure and the hybrid absorber cell . As the PZT elements couple the displacement degree of freedom (DoF) of the host to the charge displacement DoF of the shunt circuit, and MAG transducers couple the mechanical DoF of the host to the current of the shunt (i.e. the time differentiation of the charge displacement DoF), combining these two energy conversion transducers could potentially lead to a hybrid vibration absorber with an enhanced coupling factor and improved vibration attenuating performance. In this paper, a hybrid PZT-MAG Vibration Absorber (PMVA) attached to their shunt circuits is introduced for the first time and its mathematical model is derived. The parametric model of this system is introduced and the receptance function of the vibrating host is obtained. Optimum design of the shunt circuits is recommended via the minimisation of the maximum displacement amplitude of the host (so called h_∞ norm optimisation method). A four-dimensional numerical optimisation algorithm is employed to evaluate the optimum shunts based on the "*equal-peak design*" approach [9] in vibration absorbers. A comprehensive optimum designs of the current PMVA is proposed at different optimum conditions that can be used by design engineers in practical applications in vibration attenuating of structures using PMVAs.

II. Mathematical Modelling of PMVAs

The schematic of the proposed PMVA is demonstrated in Fig. 1. The single DoF vibrating host with the mass of m attached to the fixed base with the equivalent structural stiffness of k, and viscous damping c is excited by a harmonic external force $F(t)$ leading to mechanical displacement response of $x(t)$. The vibrating host is mechanically connected to a PZT and a MAG transducer each has their own resonating shunt circuit as depicted in the figure. To derive the governing equations of motion, equilibrium of dynamic forces is applied to the mass m. Balance of all forces on the mass leads to Equation (1) where $\theta = \frac{\kappa_0}{\kappa_0^2-1}\sqrt{\frac{k_P}{C}}$ is the electromechanical coupling factor of the PZT transducer with k_P and C_P as the corresponding stiffness and capacitance of the PZT element with open circuit [10] and $\kappa_0 = d_{33}\frac{1}{\sqrt{{S_{33}}^E\,{\epsilon_3}^T}}$. d_{33}, ${S_{33}}^E$ and ${\epsilon_3}^T$ are the piezoelectric constant in the axial mode (d_{33} mode), permittivity under constant stress and the compliance under constant electric field of the PZT transducer, correspondingly [9], [10], [33]. The structural stiffness of the MAG transducer is presented by k_M with the "*electro-to-mechanical*" coupled factor of $\phi = k_M\, d_{1\,M}\, N$ where $d_{1\,M}$ is defined as the piezomagnetic coefficient of the MAG element and N is the turns of wire wound in the coil of the MAG transducer [34]. Applying Kirchhoff law in the PZT and MAG resonating circuit assuming they have currents as $i_1(t)$ and $i_2(t)$ as shown in Fig. 1, lead to Equations 2 and 3, correspondingly. In Equation 2, L_P and R_P are the inductance and resistance of is the PZT shunt and voltage of $-\theta\, x(t)$ is created due to the piezoelectric properties of the PZT transducer [10]. L_M is the equivalent inductance of the MAG transducer [34], [35] and R_M and C_M present the resistance and capacitance of the MAG shunt circuit. An induced voltage due to the coupling of MAG transducer to the vibrating host is created also in this shunt (in Equation 3) proportional to the velocity of the host as $\psi\,\frac{\mathrm{d}}{\mathrm{d}t}x\,(t)$, where $\psi = k_M\, d_{2\,M}\, N$ is the "*mechanical-to-electro coupled factor*" and $d_{2\,M}$ is the piezomagnetic coefficient of the MAG element [34]. In summary, the governing equations of motion of the

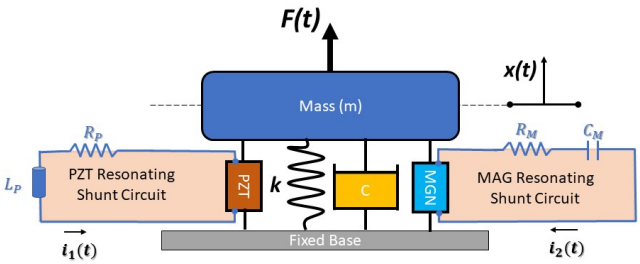

Fig. 1. The schematic of the Piezoelectric-Magnetostrictive Vibration Absorber (PMVA) attached to the vibrating host.

proposed PMVA (Figure 1) are written in the form of a three DoF system :

$$m\frac{\mathrm{d}^2}{\mathrm{d}t^2}x\left(t\right)+c\frac{\mathrm{d}}{\mathrm{d}t}x\left(t\right)+\left(k+k_M+k_P\right)x\left(t\right)+ \\ -\varphi\, i_2\left(t\right)-\theta\, q_1\left(t\right)=F\left(t\right), \tag{1}$$

$$L_P\,\frac{\mathrm{d}}{\mathrm{d}t}i_1\left(t\right)+R_P\,i_1\left(t\right)+\frac{q_1\left(t\right)}{C_P}-\theta\,x\left(t\right)=0, \tag{2}$$

$$L_M\,\frac{\mathrm{d}}{\mathrm{d}t}i_2\left(t\right)+R_M\,i_2\left(t\right)+\frac{q_2\left(t\right)}{C_M}+\psi\,\frac{\mathrm{d}}{\mathrm{d}t}x\left(t\right)=0. \tag{3}$$

where $i_1(t)=\frac{dq_1(t)}{dt}$ and $i_2(t)=\frac{dq_2(t)}{dt}$ are the currents in the PZT and MAG shunts, correspondingly with $q_1(t)$ and $q_2(t)$ demonstrating charge displacements in the commensurate shunts. Equations (1), (2) and (3) are rearranged in the following matrix form :

$$\mathbf{M}\,\ddot{\mathbf{X}}+\mathbf{C}\,\dot{\mathbf{X}}+\mathbf{K}\,\mathbf{X}=\mathbf{F}, \tag{4}$$

with the displacement vector is defined as $\mathbf{X}=\begin{bmatrix}x(t)\\q_1(t)\\q_2(t)\end{bmatrix}$, where symbol $\dot{()}$ is differentiation against time $(=d/dt)$ and the mass $\mathbf{M}$, damping $\mathbf{C}$, stiffness $\mathbf{K}$ matrix, and force vector $\mathbf{F}$ are as summarised follows:

$$\mathbf{M}=\begin{bmatrix}m&0&0\\0&L_P&0\\0&0&L_M\end{bmatrix},\quad \mathbf{C}=\begin{bmatrix}c&0&-\varphi\\0&R_P&0\\\psi&0&R_M\end{bmatrix},$$
$$\mathbf{K}=\begin{bmatrix}k_{eq}&-\theta&0\\-\theta&\frac{1}{C_P}&0\\0&0&\frac{1}{C_M}\end{bmatrix},\quad \mathbf{F}=\begin{bmatrix}F(t)\\0\\0\end{bmatrix}, \tag{5}$$

With $k_{eq}\equiv k+k_M+k_P$. It is worth highlighting that, the matrix form of the equations of motions clearly reveals the enhancement in the coupling between the structural (mechanical) displacement DoF and the electrical ones. As it can be seen, employing a PZT transducer creates a coupling in the system in the stiffness matrix $\mathbf{K}$ (via coupling factor of θ) and the MAG transducer adds extra coupling to the damping matrix $\mathbf{C}$ (via coupling factors of ψ and ϕ). As expected, a stronger dynamic coupling is created here by using the suggested PMVA.

The displacement vector $\mathbf{X}$ is transformed to the frequency domain with $\mathbf{X}\equiv\begin{bmatrix}X\\Q_1\\Q_2\end{bmatrix}\mathrm{e}^{I\,\Omega\,t}$, where $I=\sqrt{-1}$. The natural frequency of the mechanical host structure is defined as $\omega_1=\sqrt{k_{eq}/m}$ with Ω as the exciting frequency of the external harmonic load $F(t)=F_0\,\mathrm{e}^{I\,\Omega\,t}$. The amplitude of mechanical displacement of the mass is X, and the charge displacement of shunt circuit of the PZT and MAG absorber are defined as Q_1, and Q_2, correspondingly.$g=\frac{\Omega}{\omega_1}$ is defined as the exciting frequency ratio . Substituting new definition of the displacement vector $\mathbf{X}$ and $F(t)$ into Equation (4) along with the following new dimensionless parameters :

- **Mechanical degree of freedom** : Damping ratio $\zeta_1=\frac{c}{2\,m\,\omega_1}$, and $X_{st}=\frac{F_0}{k_{eq}}$
- **PZT charge degree of freedom**: Damping ratio of the shunt $r_P=R_P\,C_P\,\omega_2/2$, with frequency of $\omega_2=\frac{1}{\sqrt{C_P\,L_P}}$, frequency ratio of $\delta_P=\frac{\omega_2}{\omega_1}$ and PZT coupling coefficient $\alpha_p=\sqrt{\frac{C_P}{k_{eq}}}\theta$.
- **MAG charge degree of freedom**: Damping ratio of the shunt $r_M=R_M\,C_M\,\omega_3/2$, with frequency of $\omega_3=\frac{1}{\sqrt{C_M\,L_M}}$ and frequency ratio of $\delta_M=\frac{\omega_3}{\omega_1}$ with MAG coupling coefficient $\alpha_M=\sqrt{\frac{C_M\,\varphi\,\psi}{m}}$,

lead to the following algebraic form of the governing equations in the frequency domain:

$$[\mathbf{A}]\times\begin{bmatrix}X\\Q_1\\Q_2\end{bmatrix}=\begin{bmatrix}X_{st}\\0\\0\end{bmatrix}. \tag{6}$$

where

$$[\mathbf{A}]=\begin{bmatrix}2\,I\,g\zeta_1-g^2+1&-\frac{\theta}{k_{eq}}&\frac{-I\,g{\alpha_M}^2}{w_1\,C_2\,\psi\,{\delta_M}^2}\\-\frac{{\alpha_P}^2{\delta_P}^2k_{eq}}{\theta}&2\,I\,g\delta_P\,r_P-g^2+{\delta_P}^2&0\\I\,C_M\,g\,\psi\,w_1\,{\delta_M}^2&0&2\,I\,g\delta_M\,r_M-g^2+{\delta_M}^2\end{bmatrix}. \tag{7}$$

Equation (6) is solved for the amplitudes

$$\begin{bmatrix}X\\Q_1\\Q_2\end{bmatrix}=[\mathbf{A}]^{-1}\times\begin{bmatrix}X_{st}\\0\\0\end{bmatrix}, \tag{8}$$

and the receptance function of the mechanical DoF $G\equiv\frac{X}{X_{st}}$, as the main performance indicator of the absorber, is obtained using the solution of Equation (8) :

$$G\equiv\frac{X}{X_{st}}=\frac{NG}{DG}, \tag{9}$$

where its numerator is summarised as :

$$NG=g^4-\left(2\,I\,r_M\,\delta_M+2\,I\,r_P\,\delta_P\right)g^3 \\ -\left(4\,r_M\,r_P\,\delta_M\,\delta_P+{\delta_M}^2+{\delta_P}^2\right)g^2+ \\ +2\,I\,\delta_P\,\delta_M\,\left(r_M\,\delta_P+r_P\,\delta_M\right)g+{\delta_M}^2{\delta_P}^2, \tag{10}$$

with its denominator as :

$$DG=-g^6+\left(2\,I\,r_M\,\delta_M+2\,I\,r_p\,\delta_p\right)g^5+ \\ \left(\left({\alpha_M}^2+1\right){\delta_M}^2+4\,r_M\,r_p\,\delta_M\,\delta_p+{\delta_p}^2+1\right)g^4+ \\ \left[-2\,I\,\left({\alpha_M}^2+1\right)\delta_p\,r_p\,{\delta_M}^2-2\,ir_M\,\left({\delta_p}^2+1\right)\delta_M-2\,ir_p\,\delta_p\right]g^3+ \\ \left[\left(-1+\left(-{\alpha_M}^2-1\right){\delta_p}^2\right){\delta_M}^2-4\,r_M\,r_p\,\delta_M\,\delta_p+{\delta_p}^2\left({\alpha_p}^2-1\right)\right]g^2+ \\ -2\,I\delta_p\,\left[-r_p\,\delta_M+r_M\,\delta_p\,\left({\alpha_p}^2-1\right)\right]\delta_M\,g+\left(1-{\alpha_p}^2\right){\delta_p}^2{\delta_M}^2. \tag{11}$$

The receptance transfer function described by Equation (9) along with Equations (10) and (11), mimic the vibration level of the undamped host structure (i.e. $\zeta_1=0$) against exciting frequency ratio g based on eight design parameters including dimensionless frequency ratios of δ_P and δ_M ; damping ratios of r_P and r_M and coupling coefficients of α_P and α_M.

It is worth noting that the MAG shunt circuit can be switched off provided that $\delta_M = r_M = \alpha_M = 0$ and the receptanace transfer function of G in (9) , turns to the transfer function of the piezoelectric vibration absorbers (PVA) G_{PZT}:

$$G_{PZT} = \frac{-2\,I\,g\delta_P\,r_P + g^2 - {\delta_P}^2}{-g^4 + 2\,I\,\delta_p\,r_p\,g^3 + \left({\delta_p}^2 + 1\right)g^2 - 2\,I\,\delta_p\,r_p\,g + {\delta_p}^2\,({\alpha_p}^2 - 1)}. \tag{12}$$

Similarly, assuming parameters related to the PZT shunt circuit are ignored ($\delta_P = r_P = \alpha_P = 0$), the transfer function of the magnetorestrictive vibration absorbers (MVA) is obtained G_{MAG}:

$$G_{MAG} = \frac{-2Ig\delta_M r_M + g^2 - \delta_M^2}{\begin{bmatrix} -g^4 + 2I\delta_M\,r_M\,g^3 + (\alpha_M^2 + \delta_M^2 + 1)g^2 \\ -2I\,\delta_M\,r_M\,g - \delta_M^2 \end{bmatrix}}. \tag{13}$$

III. Performance Evaluation of PMVAs

The receptance function of the PMVAs (G), described by Equation (9), demonstrates the normalised vibration amplitude of the host X/X_{st} against the frequency of the exciting force through the dimensionless frequency ratio g. It is characterised by the coupling parameters α_P and α_M, damping parameters r_P and r_M, and frequency ratios δ_P and δ_M. The coupling parameters α_P and α_M are dependent on the energy conversion and structural characteristics of the PZT and MAG transducer and remain constant as long as the structure of the PMVA is not changed. The attenuating performance of the absorber can be altered then by changing the elements in the shunt circuits through the other four parameters (r_P, r_M, δ_P, and δ_M). As a numerical example, Figure (2) demonstrates the norm of the receptance function $|G|$ against the exciting frequency ratio g for a PMVA with $\alpha_P = 0.1$ and $\alpha_M = 0.05$; damping parameters $r_P = 0.1$ and $r_M = 0.03$; and frequency parameters of $\delta_P = \delta_M = 1$. The performance of the PMVA is compared with the corresponding performance of the PVA and MVA (when the shunt circuit of the PZT and/or MAG transducer is open, correspondingly). As expected, the figure clearly shows that the damping performance of the PMVA is much better than the other two absorbers. While both resonating shunts are active, energy conversion between the mechanical DoF and electric shunt circuits is enhanced, leading to a lower maximum vibration amplitude of the PMVA compared to the PVA and MVA. However, the maximum amplitude of the PMVA can still be smaller and the performance can be enhanced and optimised by proper choice of the four design parameters δ_P, δ_M, r_P and r_M. Figures (3) reveal the importance of the optimum shunt design in PMVAs and demonstrate that any slight change(s) in any of these parameters might lead to a catastrophic performance deterioration of the absorber. A precise optimisation needs to be conducted to ensure that the optimum performances of the PMVAs are achieved and maximum vibration attenuation is occurred.

IV. Tuning and Optimisation of PMVAs

In this research, minimisation of the maximum vibration amplitudes of the host structure (so called h_∞ optimisation technique) is employed numerically to obtain the optimum design of the shunt circuits, through finding optimal parameters of the system (i.e. $\delta_{P\,opt}, \delta_{M\,opt}, r_{P\,opt}$ and $r_{M\,opt}$) at a given values of α_P and α_M . A four-dimensional numerical optimisation algorithm is employed to satisfy the following objective function and identify the corresponding optimum parameters :

$$Max|G(g, \delta_{P\,opt}, \delta_{M\,opt}, r_{P\,opt}, r_{M\,opt})| = min(Max_{\delta_P, \delta_M, r_P, r_M}|G(g)|). \tag{14}$$

Table I lists the h_∞ optimum values of the PVA, MVA and PMVA for a given $\alpha_P = 0.1$ and $\alpha_M = 0.05$ using this optimisation algorithm. The corresponding tuned response of each absorber is also plotted in Figure (4) next to their detuned

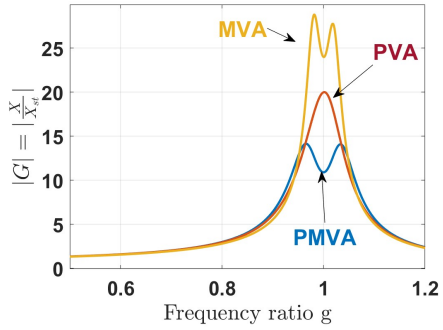

Fig. 2. Vibration response of the host structure (normalised amplitude) against exciting frequency ration g for a PMVA with $\alpha_P = 0.1$, $\alpha_M = 0.05$, $r_P = 0.1$, $r_M = 0.03$, $\delta_P = \delta_M = 1$; compared to the PVA and MVA with similar corresponding relevant parameters.

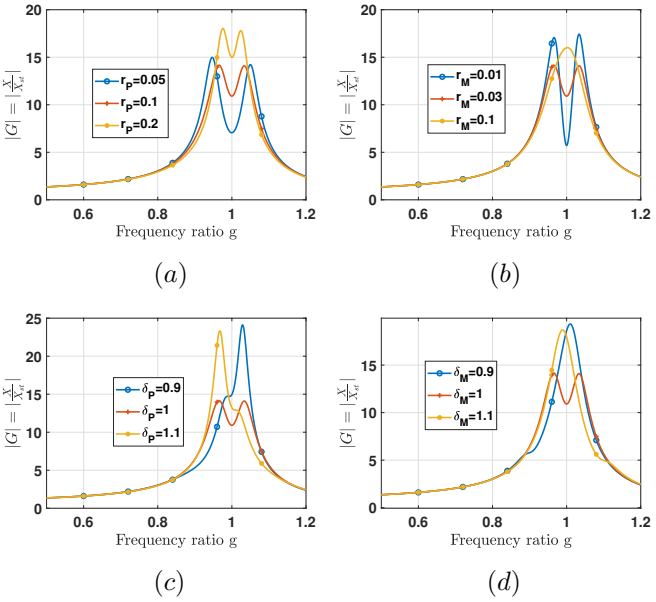

Fig. 3. Variations of the normalised vibration amplitude ($|G|$) for a PMVA ($\alpha_P = 0.1$, $\alpha_M = 0.05$, $r_P = 0.1$, $r_M = 0.03$, and $\delta_P = \delta_M = 1$) with changes in (a) r_P, (b) r_M, (c) δ_P and (d) δ_M .

responses (already plotted in Figure (2)). It is seen from this figure that all absorbers (PVA,MVA and PMVA) are fully tuned as their frequency responses have resonance peaks with equal heights (so called the equal-peak design [2], [10]) and also in each specific absorber, the maximum height of the detuned response is lower than the maximum height of the detuned one. However, comparing the maximum height h_{max} of the tuned absorbers shows that the attenuating performance of the introduced PMVA at the current coupling factors (i.e. $\alpha_P = 0.1$ and $\alpha_M = 0.05$) are significantly enhanced compared to the performances of the similar tuned PVA and/ or MVA. The dimensionless maximum vibration amplitude at the resonant peaks of the tuned MPVA is 19% and 59% lower than the tuned PVA and tuned MVA, correspondingly. This significant enhancement in the performance of the PMVA confirms that a higher dynamic electromechanical coupling is achieved in the proposed PMVA, leading to an improved attenuating performance compares to the similar tuned PVA and MVA.

TABLE I
OPTIMUM PARAMETERS FOR A PVA, MVA AND PMVA BASED ON h_∞ OPTIMISATION.

$\alpha_P = 0.1$	**Optimum parameters**				
$\alpha_M = 0.05$	$\delta_{P\,opt}$	$\delta_{M\,opt}$	$r_{P\,opt}$	$r_{M\,opt}$	h_{max}
tuned PVA	1.00	NA	0.0615	NA	14.162
tuned MVA	NA	0.994	NA	0.0306	28.3
tuned PMVA	0.9811	1.038	0.0622	0.0362	11.4616

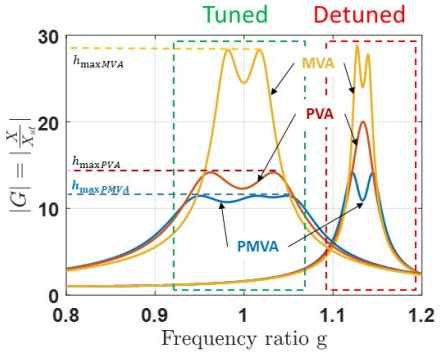

Fig. 4. Vibration behaviour of the host structure coupled to a tuned absorber (PMVA, PVA, and MVA with optimum parameters given in Table(I)) in comparison to the detuned one defined in Figure (2).

To obtain a wider range of optimum designs of the PMVAs, the developed optimisation algorithm based on h_∞ approach employed for various values of the magnetorestrictive coupling factor α_M at the constant $\alpha_P = 0.1$ and optimum parameters of the system are calculated. Variation of all these four optimum parameters are plotted in Figures (5). These optimum data can be used in design of shunt circuits of PMVAs at different α_M. Variations of the maximum height of the resonance peaks in the host dimensionless vibration amplitude $h_{max\,opt}$) is plotted against α_M in Figure(6) and as expected, the vibration amplitude of the host at resonance drops with the coupling factor of α_M at constant $\alpha_P = 0.1$. To demonstrate the accuracy of the proposed optimised solution, optimum parameters at four different $\alpha_M s$,suggested by Figures (5), are employed and their corresponding frequency responses are plotted in Figure (7) . All PMVAs are showing a tuned frequency response with the resonance peaks of exactly the same height h_{max}. However, h_{max} drops with α_M as it was already revealed in Figure (6) . At higher values of α_M, three resonance peaks with the same height are observed (instead of two) , clearly highlights that at higher dynamic coupling factor all three dynamic systems (i.e. the vibrating host structures , and also the PZT and MAG shunt circuits) are heavily coupled and are fully resonating, leading to an enhanced energy transfer between DoFs and improving the performances of the PMVA absorber, correspondingly.

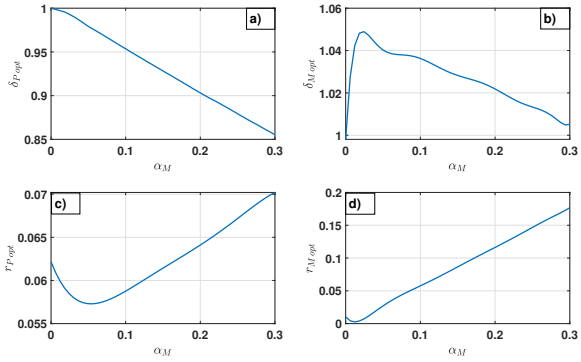

Fig. 5. Optimum parameters [(a) δ_P (b) δ_M (c) r_P and (d) r_M] of a tuned PMVA with $\alpha_P = 0.1$ against α_M based on h_∞ optimisation and equal-peak method.

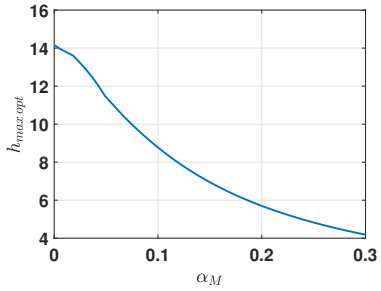

Fig. 6. Optimum height of the resonance peaks of a PMVA with $\alpha_P = 0.1$ against α_M.

V. CONCLUSION

In this research, a new hybrid piezoelectric-magnetostrictive vibration absorbers (PMVA) is introduced. A PZT transducer attached to a resonating shunt is coupled to a one DoF vibrating host in parallel with a MAG transducer attached to the second resonating shunt. The PZT couples the displacement of the host to the charge displacement of the shunt while MAG creates a coupling between the velocity of the host and the current of the shunt. A stronger dynamic coupling

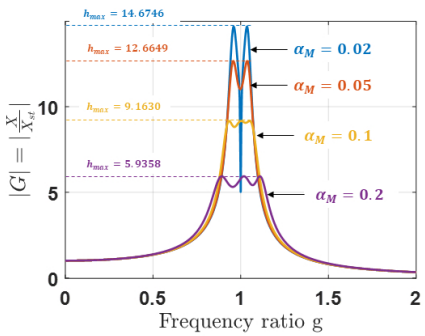

Fig. 7. Equal peak design of a PMVA with $\alpha_P = 0.1$ and different α_M according to the h_∞ optimisation.

is created between the mechanical and electrical DoFs in PMVAs in comparison to the traditionally used PVA and MVA. The governing equations of this new hybrid absorber is also derived and mathematical dimensionless model is developed. To optimise the receptance function of the absorbers in the frequency domain, h_∞ norm optimisation is employed through a four-dimensional optimisation algorithm. The optimised parameters of the shunts are calculated to achieve the equal-peak criterion. A significant enhancement in absorber performance of the PMVA (minimum 19% up to 59% improvement) is observed in comparison to the PVA and/or MVA with the similar structural condition. A series of optimum designs at different MAG coupling factors are obtained to be used for tuning the PMVA shunts in practical conditions. It is also demonstrated that these optimum designs accurately tune the frequency response of the host structure with equal heights at their resonance peaks and at the lowest possible displacement amplitude of the host.

REFERENCES

[1] A. Deraemaeker and P. Soltani, "A short note on equal peak design for the pendulum tuned mass dampers (vol 231, pg 285, 2017)," *PROCEEDINGS OF THE INSTITUTION OF MECHANICAL ENGINEERS PART K-JOURNAL OF MULTI-BODY DYNAMICS*, vol. 235, no. 3, pp. 536–536, 2021.

[2] P. Soltani and A. Deraemaeker, "Pendulum tuned mass dampers and tuned mass dampers: Analogy and optimum parameters for various combinations of response and excitation parameters," *Journal of vibration and control*, vol. 28, no. 15-16, pp. 2004–2019, 2022.

[3] Y. Younes, M. Younes *et al.*, "An experimental study on the damping characteristics and tuning of the liquid column vibration absorber," in *Journal of Physics: Conference Series*, vol. 2299, no. 1. IOP Publishing, 2022, p. 012007.

[4] B. Mehrkian and O. Altay, "Omnidirectional liquid column vibration absorbers for multi-story buildings," *Journal of Building Engineering*, vol. 62, p. 105306, 2022.

[5] B. Yu and A. Luo, "Steady state performance of a nonlinear vibration absorber on vibration reduction of a harmonically forced oscillator," *The European Physical Journal Special Topics*, vol. 228, pp. 1823–1837, 2019.

[6] S. Elias, R. Rupakhety, D. De Domenico, and S. Olafsson, "Seismic response control of bridges with nonlinear tuned vibration absorbers," in *Structures*, vol. 34. Elsevier, 2021, pp. 262–274.

[7] G. M. Stewart, "Load reduction of floating wind turbines using tuned mass dampers," 2012.

[8] S. Kopylov, Z. Chen, and M. A. Abdelkareem, "Implementation of an electromagnetic regenerative tuned mass damper in a vehicle suspension system," *IEEE Access*, vol. 8, pp. 110 153–110 163, 2020.

[9] P. SOLTANI, G. Tondreau, A. Deraemaeker, and G. Kerschen, "Linear and nonlinear piezoelectric shunting strategies for vibration mitigation," in *MATEC Web of Conferences*, vol. 16. EDP Sciences, 2014, p. 01007.

[10] P. Soltani, G. Kerschen, G. Tondreau, and A. Deraemaeker, "Piezoelectric vibration damping using resonant shunt circuits: an exact solution," *Smart Materials and Structures*, vol. 23, 2014.

[11] A. Presas, Y. Luo, Z. Wang, D. Valentin, and M. Egusquiza, "A review of pzt patches applications in submerged systems," *Sensors*, vol. 18, no. 7, p. 2251, 2018.

[12] X. Jiao, J. Zhang, W. Li, Y. Wang, W. Ma, and Y. Zhao, "Advances in spacecraft micro-vibration suppression methods," *Progress in Aerospace Sciences*, vol. 138, p. 100898, 2023.

[13] T. Sales, D. Rade, and L. De Souza, "Passive vibration control of flexible spacecraft using shunted piezoelectric transducers," *Aerospace Science and Technology*, vol. 29, no. 1, pp. 403–412, 2013.

[14] H. Sun, Z. Yang, K. Li, B. Li, J. Xie, D. Wu, and L. Zhang, "Vibration suppression of a hard disk driver actuator arm using piezoelectric shunt damping with a topology-optimized pzt transducer," *Smart Materials and Structures*, vol. 18, no. 6, p. 065010, 2009.

[15] S. Venna and Y.-J. Lin, "An effective approach for optimal pzt vibration absorber placement on composite structures," 2013.

[16] Y. Abdullah and A. Baz, "Brake squeal: A control strategy using shunted piezoelectric pads," *Journal of Vibration and Acoustics*, vol. 143, no. 3, 2021.

[17] J.-j. Wei, Z.-c. Qiu, J.-d. Han, and Y.-c. Wang, "Experimental comparison research on active vibration control for flexible piezoelectric manipulator using fuzzy controller," *Journal of Intelligent and Robotic Systems*, vol. 59, pp. 31–56, 2010.

[18] K. Marakakis, G. K. Tairidis, P. Koutsianitis, and G. E. Stavroulakis, "Shunt piezoelectric systems for noise and vibration control: a review," *Frontiers in Built Environment*, vol. 5, p. 64, 2019.

[19] A. L. Araújo and J. F. Aguilar Madeira, "Optimal passive shunted damping configurations for noise reduction in sandwich panels," *Journal of Vibration and Control*, vol. 26, no. 13-14, pp. 1110–1118, 2020.

[20] X. Liu, C. Wang, Y. Zhang, K. Wu, B. Dong, and L. Huang, "Extra sound attenuation via shunted piezoelectric resonators in a duct," *International Journal of Mechanical Sciences*, vol. 225, p. 107370, 2022.

[21] S. R. Marjani and D. Younesian, "Performance analysis of piezoelectric actuators in railway wheel squealing noise mitigation," *Shock and Vibration*, vol. 2019, pp. 1–13, 2019.

[22] S. Talebian, Y. Hojjat, M. Ghodsi, M. R. Karafi, and S. Mirzamohammadi, "A combined preisach–hyperbolic tangent model for magnetic hysteresis of terfenol-d," *Journal of Magnetism and Magnetic Materials*, vol. 396, pp. 38–47, 2015.

[23] S. Talebian, Y. Hojjat, M. Ghodsi, and M. R. Karafi, "Study on classical and excess eddy currents losses of terfenol-d," *Journal of Magnetism and Magnetic Materials*, vol. 388, pp. 150–159, 2015.

[24] S. Mirzamohamadi, M. M. Sheikhi, M. R. Karafi, M. Ghodsi, and S. Ghorbanirezaei, "Novel contactless hybrid static magnetostrictive force-torque (chsmft) sensor using galfenol," *Journal of Magnetism and Magnetic Materials*, vol. 553, p. 168969, 2022.

[25] M. Ghodsi, M. Modabberifar, and T. Ueno, "Quality factor, static and dynamic responses of miniature galfenol actuator at wide range of temperature," *International Journal of Physical Sciences*, vol. 6, no. 36, pp. 8143–8150, 2011.

[26] Z. Deng and M. J. Dapino, "Review of magnetostrictive materials for structural vibration control," *Smart Materials and Structures*, vol. 27, no. 11, p. 113001, 2018.

[27] M. Ghodsi, M. Mohammadzaheri, P. Soltani, and H. Ziaifar, "A new active anti-vibration system using a magnetostrictive bimetal actuator," *Journal of Magnetism and Magnetic Materials*, vol. 557, p. 169463, 2022.

[28] Z. Deng, J. J. Scheidler, V. M. Asnani, and M. J. Dapino, "Shunted magnetostrictive devices in vibration control," *Smart Materials and Structures*, vol. 29, no. 10, p. 105007, 2020.

[29] J. J. Scheidler and V. M. Asnani, "Validated linear dynamic model of electrically-shunted magnetostrictive transducers with application to structural vibration control," *Smart Materials and Structures*, vol. 26, no. 3, p. 035057, 2017.

[30] Z. Deng, V. M. Asnani, and M. J. Dapino, "Magnetostrictive vibration damper and energy harvester for rotating machinery," in *Industrial and*

Commercial Applications of Smart Structures Technologies 2015, vol. 9433. SPIE, 2015, pp. 84–94.

[31] P. Martynowicz, "Nonlinear optimal-based vibration control of a wind turbine tower using hybrid vs. magnetorheological tuned vibration absorber," *Energies*, vol. 14, no. 16, p. 5145, 2021.

[32] X. Wang, H. Wu, and B. Yang, "Micro-vibration suppressing using electromagnetic absorber and magnetostrictive isolator combined platform," *Mechanical Systems and Signal Processing*, vol. 139, p. 106606, 2020.

[33] P. Soltani, G. Kerschen, G. Tondreau, and A. Deraemaeker, "Tuning of a piezoelectric vibration absorber attached to a damped structure," *Journal of Intelligent Material Systems and Structures*, vol. 28, no. 9, pp. 1115–1129, 2017.

[34] S. Cao, X. Yue, J. Zheng, C. Liu, J. Zhao, and Y. Li, "Dynamic coupled model of vibration system with galfenol damper considering eddy currents and hysteresis," *IEEE Transactions on Magnetics*, vol. 56, no. 1, pp. 1–4, 2019.

[35] S. Cao, L. Liu, J. Zheng, R. Pan, and G. Song, "Modeling and analysis of galfenol nonlinear cantilever energy harvester with elastic magnifier," *IEEE Transactions on Magnetics*, vol. 55, no. 6, pp. 1–5, 2019.